An undergraduate experiment on x-ray spectra and Moseley's law using a scanning electron microscope

C. W. S. Conover and John Dudek[a)]
Department of Physics, Colby College, Waterville, Maine 04901

(Received 6 February 1995; accepted 29 June 1995)

We describe an undergraduate laboratory experiment developed for sophomore modern physics students, using the x-ray analysis feature of a scanning electron microscope. The experiment described is a fundamental physics measurement performed with a state-of-the-art apparatus not usually used in pedagogical physics experiments. The characteristic x-ray spectrum of elements shows a simple progression that can be quantitatively explained by the conceptually important Bohr–Rutherford shell model of atomic structure. Students measure the $K\alpha$ and $K\beta$ x-ray spectra from metals in the range of $12 \leqslant Z \leqslant 41$. The measurements allow the verification of Moseley's law scaling of x-ray energies with atomic number and a quantitative measure of the data's fit to the shell model. © *1996 American Association of Physics Teachers.*

I. INTRODUCTION

A large number of experiments have recently been described in the fields of atomic and condensed matter physics which use modern research equipment to explore basic physical principles, see, e.g., Refs. 1–4. Much sophisticated apparatus originally invented by physicists is currently used both in research and in undergraduate laboratory experiments in disciplines other than physics. Obvious examples of such apparatus are NMR spectrometers, scanning and transmission electron microscopes, x-ray diffractometers, and Fourier-transform-infrared spectrometers. Such apparatus is regularly used for undergraduate experiments in biology, chemistry, and geology. The use of such equipment in the laboratory component of a modern physics class allows a middle path between physics research equipment and student laboratories. The data acquired with these devices are usually convincing, since the systems that physicists study are usually much more clean than those for which the instruments are designed.

As a model for such experiments, we report the development of a laboratory for use in a sophomore level modern physics class using a scanning electron microscope with an x-ray detection system. The experiment involves taking several photographs with an electron microscope, followed by measurements of the x-ray spectra of several elements and analysis of the variation of the x-ray spectra with atomic number. The laboratory is straightforward to perform and the data are convincing.

II. BACKGROUND FOR THE X-RAY EXPERIMENT

In 1913 Bragg discovered that different elements produced characteristic x-ray lines when bombarded with energetic electrons. A systematic study of these characteristic x-ray lines was performed by Moseley in 1913–1914,[5–9] who discovered that, although the optical spectra of atoms are extraordinarily complicated, the x-ray spectra of different elements progress in a simple way. When different targets are bombarded with energetic electrons, there are two prominent series of x-ray lines, denoted the K and L series, each of which shifts regularly to higher frequency as the atomic number, Z, of the target is increased. The energies of the x-ray spectra can all be fit to a function of the form

$$E = h\nu = B(Z-\sigma)^2, \tag{1}$$

where B and σ depend on the family of x-ray lines. B is on the order of the Rydberg energy and σ is now understood to be a "screening parameter" (discussed further below) due to other inner shell electrons. For the highest energy (K series) x-ray lines, the numerical value of σ is approximately 1, but is somewhat larger for the lower energy series. Equation (1) is referred to as Moseley's law.

Roughly at the same time as Moseley's experiments, Bohr predicted the hydrogenic energy levels of a single electron orbiting a nucleus of charge $+Z$. The Bohr equation for hydrogenic transition energies, E, is

$$E = R\left(\frac{1}{n_f^2} - \frac{1}{n_i^2}\right)Z^2, \tag{2}$$

where R is the Rydberg constant, and n_i and n_f are the principal quantum numbers of the initial and final atomic states. The hydrogenic model of the energy levels predicts the Z dependence of Moseley's law, but only if Z is replaced by an effective nuclear charge, $(Z-\sigma)$, as seen in Eq. (1). The great success of the Bohr–Rutherford model is its prediction of the values of B in Eq. (1) for the different series; each x-ray series can easily be assigned an initial and a final state.

It is now understood that the characteristic x-ray lines are due to inner shell processes in atoms. If an electron impact removes, for example, an electron from the innermost shell, electrons from higher levels can make a transition into that shell and emit an x-ray photon. The transition from the $n=2$ shell to the $n=1$ shell emits x rays of the $K\alpha$ line, and atoms making $n=3$ to $n=1$ transitions emit the x rays of the $K\beta$ line. The factor $(Z-\sigma)$ for the x-ray transitions is explained by a screening of part of the nuclear charge by the inner shell electrons which have not been removed. For $K\alpha$ lines a very good estimate of σ can be made. Since the $n=1$ shell normally contains two electrons, when one electron has been removed the field of the nucleus is screened by the remaining electron. Thus, the "effective nuclear charge" seen by the electron in the $n=2$ shell is $Z-1$, and the screening parameter, σ, for the $K\alpha$ line is predicted to be 1. In transitions from $n=3$ to $n=1$ the screening parameter is obviously larger, but difficult to determine *a priori*.

Moseley's work was the first to give a firm meaning to the concept of atomic number as distinct from atomic mass and

confirmed the shell model of the atom. While the location of an element on the periodic chart generally progresses with atomic mass, the atomic mass of argon ($Z=18$) is larger than that of potassium ($Z=19$) [cobalt ($Z=27$) is heavier than nickel ($Z=28$), also]. These two elements had been inverted from the usual progression of atomic masses on the periodic chart to keep them in the groups corresponding to their chemical properties. Moseley's experiments gave a sound physical justification for the ad hoc inversion; a periodic chart progressing by nuclear charge, Z, places all of the elements in the correct location.

III. EXPERIMENT

Many modern electron microscopes allow the energy analysis of photons emitted from a sample. The experiments described below are performed with a Hitachi S-2700 scanning electron microscope (SEM), which can produce an electron beam from 10 to 30 keV in energy and can detect reflected or secondary electrons and x-ray photons emitted from the surface of any sample. Imaging is performed by scanning an electron beam across the surface of a sample and detecting the reflected electrons. The x rays produced due to electron impact ionization are detected with a Si(Li) detector with a beryllium window. On the S-2700 SEM the x-ray energy analysis is usually used to determine the elemental composition of an unknown sample, but in our case, the elemental composition of the sample is known and the x-ray energies are determined experimentally.

With a 30 keV beam, it is energetically possible to remove K-shell electrons out to approximately $Z=47$. However, because the cross section for removal of these tightly bound electrons falls off rapidly with increasing Z, the L series dominates the x-ray spectrum for Z in this region. We have found that the highest $K\alpha$ line that can be measured reliably with a 30 keV electron beam in our microscope corresponds to $Z=41$, with a $K\alpha$ energy of 16.6 keV; however, even at this atomic number, the spectrum is dominated by L shell x rays. The Si(Li) detector detects a charge pulse of electrons liberated by a high-energy particle passing through it; the total charge is proportional to the particle's energy. The Si(Li) detector used has a resolution of approximately 170 eV, which precludes measuring the fine structure of the x-ray spectra. The window material determines the lower energy limit for detection of x-ray photons, about 1 keV, setting the lower limit of measured spectra at Na ($Z=11$).

The sample used in this experiment is a multielement standard,[10] which is normally used for calibrating the x-ray spectrometer. The data acquisition requires taking an image of only one sample on the multielement standard, and then switching from imaging to x-ray analysis. We run the x-ray analysis software in its most elementary mode. In this mode the data acquisition system produces a histogram of number of x-ray photons detected versus photon energy. The plots can be printed easily and the peak position can be either read off the paper copy or using a cursor on a computer screen.

The first part of a laboratory session allows the students to familiarize themselves with the microscope operation by taking a photograph of an object which they bring into the laboratory. The acquisition of K-shell x-ray data is straightforward. Once the multielement standard sample is placed in the vacuum chamber of the microscope, an image is taken and data acquisition takes place at a rapid pace. Recording spectra for the approximately 15 different elements used takes slightly more than 1 h. The chosen elemental target is then moved into the center of the field of view and the magnification is increased until there is only one sample in the field of view, and a spectrum is taken using the software. At the time of acquisition spectra are printed and the energies of the major x-ray peaks are recorded.

Table I. The x-ray energies for the elements measured with the Hitachi S-2700 scanning electron microscope's elemental analysis feature. For those elements marked with an asterisk, the $K\alpha$ and $K\beta$ energies are indistinguishable within the 170 eV resolution of the detector.

Element	Atomic number	$K\alpha$ energy (keV)	$K\beta$ energy (keV)
Mg*	12	1.16	1.16
Al*	13	1.49	1.49
Si*	14	1.72	1.72
S	16	2.28	2.46
Ti	22	4.52	4.94
V	23	4.96	5.43
Cr	24	5.42	5.95
Mn	25	5.91	6.51
Co	27	6.90	7.67
Ni	28	7.49	8.26
Cu	29	8.07	8.91
Ga	31	9.24	10.28
As	33	10.52	11.7
Y	39	14.95	16.78
Zr	40	15.80	17.70
Nb	41	16.60	18.65

IV. ANALYSIS AND RESULTS

The K-shell x-ray energies for various elements are presented in Table I. For Z less than 16 we are unable to resolve the separation between the $K\alpha$ and $K\beta$ lines. The energy uncertainty is taken as a constant 170 eV for all of the energies measured.

There are several different ways to approach the analysis of the data. A possible method is to present the data initially as an unknown function of either the atomic number, Z, or atomic weight, A. Figure 1 shows a plot of $\ln(E_{K\alpha})$ vs $\ln(A)$ and $\ln(Z)$, demonstrating a linear relationship with a slope of approximately two, indicating a quadratic relationship between the $K\alpha$ energy and either the atomic number or atomic mass. However, the fit, as determined either by eye or with a χ^2 test shows that the $K\alpha$ energy is more appropriately described as a function of Z. The fortuitous linear fit to the atomic mass results from the fact that A is a slowly varying function of Z in the range of nuclei studied. Since the dependence is on $(Z-\sigma)^2$, rather than on Z^2, the slope should not be exactly two for either plot.

Once the functional form of the data is determined, it is a straightforward step to make a "Moseley plot," the square root of x-ray energy (or frequency) versus Z, of the data, using Eq. (1) in the form

$$\sqrt{E}=\sqrt{B}(Z-\sigma), \tag{3}$$

which gives a linear relationship between the measured quantity, $\sqrt{E}$, and the atomic number, Z. The line described by Eq. (3) has a slope $\sqrt{B}$ and a Z intercept of σ. Linear fits to the data, taking the energy uncertainty into account, give the slope and Z intercept of the data along with their uncertainties.[11]

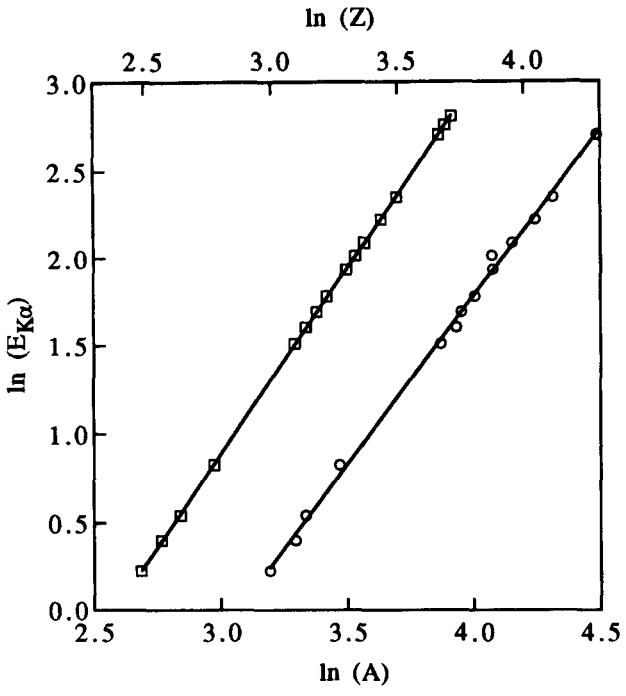

Fig. 1. Logarithmic plot of the data, showing the natural logarithm of the $K\alpha$ energies (□) vs the natural logarithmic of the atomic number, Z, and (○) vs the logarithm of the atomic mass, A. The lines shown are least-squares fits to the data. The slope of the fit to Z is 2.11 ± 0.03 and the slope of the fit to A is 1.91 ± 0.02.

Moseley plots of the data from Table I are shown in Fig. 2 for both the $K\alpha$ and $K\beta$ x-ray spectra. Linear least-squares fits to the data shown in Fig. 2 provide the parameters B and σ of Eqs. (1) and (3) for the $K\alpha$ and $K\beta$ x-ray series

$$\begin{aligned} B_{K\alpha}&=10.5\pm0.4 \text{ eV},\\ \sigma_{K\alpha}&=1.2\pm0.5,\\ B_{K\beta}&=12.2\pm0.3 \text{ eV},\\ \sigma_{K\beta}&=1.9\pm0.4. \end{aligned} \tag{4}$$

The constants predicted by the Bohr theory are $B_{K\alpha}=10.20$ eV and $B_{K\beta}=12.09$ eV. The screening parameters are both close to one, but the $K\beta$ screening parameter is larger, as is expected. As can be seen both in the numbers tabulated above and in the fitted curves shown in Fig. 2, the Bohr–Rutherford model describes the data quite accurately.

V. CONCLUSION

We have developed an experiment that allows students to use state-of-the-art equipment to perform a classic physics experiment, verification of Moseley's law, which states that the energy of x rays, E, is proportional to the square of the atomic number minus a screening factor. These results allow for a straightforward physical interpretation of the structure of atomic energy levels in terms of shells. The experiment shows that the highest energy x rays from the target elements in the range $12\leqslant Z\leqslant 41$ possess energies that are predicted by the Bohr theory of hydrogen, as long as a screening parameter is included in the energy equation.

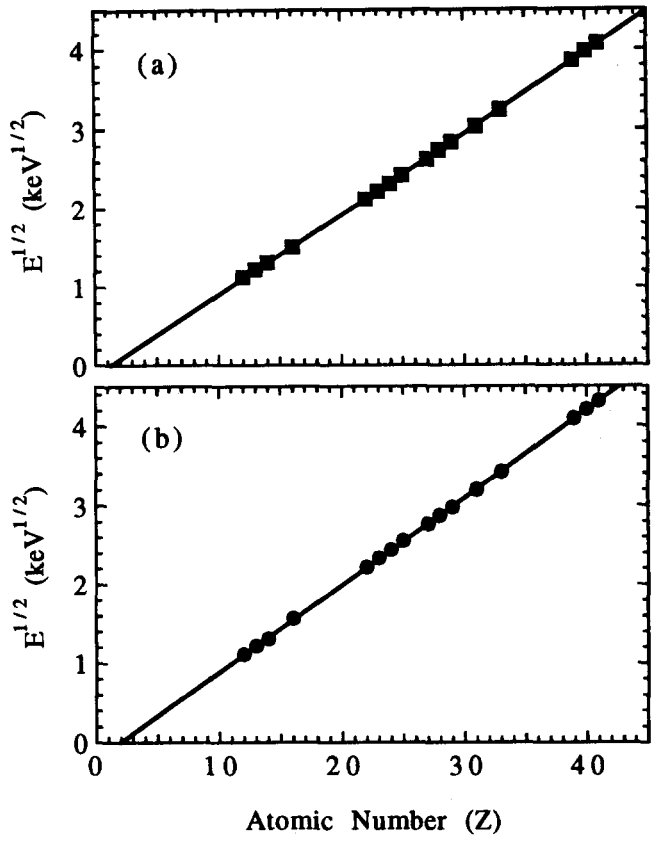

Fig. 2. Moseley plots of the (a) K_α and (b) K_β x-ray energies as a function of atomic number. Error bars are slightly smaller than the markers in the plot. The lines shown are least-squares fits to the data.

L-shell x-ray spectra can also be analyzed in a straightforward manner. A complete understanding of the L series is not possible with as simple a model as we have used. An extension to these experiments would be to use the x-ray spectrometer to determine the elemental makeup of an unknown material.

ACKNOWLEDGMENTS

It is a pleasure to acknowledge many stimulating conversations with, and assistance from, Thomas Shattuck. We would also like to thank Robert Bluhm and Richard Wolfson for a critical reading of the text and many helpful suggestions. The data presented were taken by students in PH242, spring 1994. The Hitachi S-2700 electron microscope was purchased with a generous grant from the Kresge foundation.

[a]Current address: Department of Chemistry, Princeton University, Princeton, NJ.

[1]J. C. Camparo, and C. M. Klimcak, "Laser spectroscopy on a 'shoestring,' " Am. J. Phys. **51**(12), 1077–1081 (1983).
[2]S. H. Ratcliff, D. K. Noss, J. S. Dunham, E. B. Anthony, J. H. Cooley, and A. Alvarez, "High-resolution solar spectroscopy in the undergraduate physics laboratory," Am. J. Phys. **60**, 645–649 (1992).
[3]K. B. MacAdam, A. Steinbach, and C. Wieman, "A narrow-band tunable diode laser system with grating feedback, and a saturated absorption spectrometer for Cs and Rb," Am. J. Phys. **60**(7), 1098–1111 (1992).
[4]J. M. Essick and R. T. Mather, "Characterization of a bulk semiconductors's band gap via a near absorption edge optical transmission experiment," Am. J. Phys. **61**(7), 646–649 (1993).
[5]Paul A. Tipler, *Modern Physics* (Worth, New York, 1978).

[6]R. Eisberg and R. Resnick, *Quantum Physics of Atoms, Molecules, Solids, Nuclei, and Particles* (Wiley, New York, 1985).
[7]F. K. Richtmyer, *Introduction to Modern Physics* (McGraw-Hill, New York, 1928), 1st ed.; F. K. Richtmyer, E. H. Kennard, and J. N. Cooper, *Introduction to Modern Physics* (McGraw-Hill, New York, 1969), 6th ed.
[8]H. G. J. Moseley, Philos. Mag. **26**, 1024 (1913); **27**, 703 (1914).
[9]G. Holton and D. H. D. Roller, *Foundations of Modern Physical Science* (Addison-Wesley, Reading, MA, 1958).
[10]C. M. Taylor Corporation, 289 Leota Avenue, Sunnyvale, CA 94086. Multielement Standard No. 202-52.
[11]H. D. Young, *Statistical Treatment of Experimental Data* (McGraw-Hill, New York, 1962).

The libration limits of the elastic pendulum

D. M. Davidović
The Institute Vinča, Belgrade, Yugoslavia

B. A. Aničin
Faculty of Mechanical Engineering, The University of Belgrade, Belgrade, Yugoslavia

V. M. Babović
The Faculty of Science, Physics Department, The University of Kragujevac, Kragujevac, Yugoslavia

(Received 27 July 1994; accepted for publication 2 June 1995)

The motion of the elastic pendulum is ruled by coupling between the pendulum mode and the harmonic oscillator mode. The bob of the pendulum executes trajectories in a domain of the vertical plane, the shape and size of which are set by the initial conditions and the total energy of the pendulum. The limits of this libration, in exact resonance, are studied using parabolic coordinates. Other Hamiltonians, with similar interaction terms, exhibit similar libration limits. © *1995 American Association of Physics Teachers.*

I. INTRODUCTION

The elastic, or extensible, pendulum is a simple pendulum with a spring incorporated in its string. A very complete paper on the subject was written by Vitt and Gorelik,[1] following an initiative by the Russian academician Mandel'shtam to study this case as an analog of Fermi resonance in the infrared spectrum of CO_2. Written in Russian, with an abstract in German, the paper was more frequently quoted and misquoted than read by other authors. In actual fact, the paper contains a complete description of the recurrence phenomenon, the corresponding theory of slowly varying amplitudes, the discovery of two simple parabolic orbits, the action-angle variable theory of the pendulum and an experiment, where the motion of the projection of the bob on a wall was studied and the recurrence times determined.

In general, if the bob of the electric pendulum is either raised or lowered, vertical vibrations are normally maintained. Their stability is only lost due to parametric resonance, which occurs when the harmonic oscillator frequency is twice (or nearly twice) the pendulum frequency. Under those circumstances, any small initial deviation of the bob from the vertical line passing through the spring support grows exponentially at first. This growth stops eventually, when most of the energy of the vertical pump is converted into the energy of the horizontal pendulum oscillations. The process is now reversed as the centrifugal force, with two cycles of oscillation in the pendulum period, acts as a forcing term, or subharmonic pump, to the vertical harmonic vibrations, which now build up until the initial state is restored, starting a new cycle of the recurrence process. The recurrence process does not occur when the bob moves along one of the two parabolas originally discovered by Vitt and Gorelik.[1]

The linear, or Floquet, theory of the elastic pendulum was dealt with by Olsson[2] and Aničin, Davidović, and Babović.[3] The main result is that only one parametric resonance exists, contrary to an assumption by Vitt and Gorelik,[1] according to which all integral ratios of the harmonic oscillator and pendulum frequencies should lead to resonance.

The elastic pendulum was studied many times as a teaching device, due to the importance of parametric resonance and wave–wave coupling in accelerators, electronics, plasma physics, and nonlinear optics. Cayton[4] studied the theory of the pendulum and noticed that subsequent swings occur in different planes. Lipham and Pollak[5] discussed the impact of the finite mass of the spring on the experiment. Falk[6,7] conducted a multiple time scale analysis and described student experiments with the spring pendulum. Rusbridge,[8] apart from slow-amplitude theory and computation, covered motion off exact resonance and the effect of damping. The paper also contains the description of a very interesting experiment, with a battery and light bulb on the moving weight. This allowed one to photograph the motion, during several cycles of the recurrence process, with an open camera. Two basic types of motion were recorded. Trajectories issuing from the vicinity of the origin, with a nearly vertical velocity, however complicated, are restrained to a lemonlike area, basically bound by two counter-oriented parabolas. Trajectories close to the Vitt and Gorelik parabolas cover a crescentlike area, bound essentially by two parabolas of the same orientation. The stability of the plane containing the motion was

